



Since January 2020 Elsevier has created a COVID-19 resource centre with free information in English and Mandarin on the novel coronavirus COVID-19. The COVID-19 resource centre is hosted on Elsevier Connect, the company's public news and information website.

Elsevier hereby grants permission to make all its COVID-19-related research that is available on the COVID-19 resource centre - including this research content - immediately available in PubMed Central and other publicly funded repositories, such as the WHO COVID database with rights for unrestricted research re-use and analyses in any form or by any means with acknowledgement of the original source. These permissions are granted for free by Elsevier for as long as the COVID-19 resource centre remains active.

# Effects of human mobility restrictions on the spread of COVID-19 in Shenzhen, China: a modelling study using mobile phone data



Ying Zhou, Renzhe Xu, Dongsheng Hu, Yang Yue, Qingquan Li, Jizhe Xia



## Summary

**Background** Restricting human mobility is an effective strategy used to control disease spread. However, whether mobility restriction is a proportional response to control the ongoing COVID-19 pandemic is unclear. We aimed to develop a model that can quantify the potential effects of various intracity mobility restrictions on the spread of COVID-19.

**Methods** In this modelling study, we used anonymous and aggregated mobile phone sightings data to build a susceptible–exposed–infectious–recovered transmission model for COVID-19 based on the city of Shenzhen, China. We simulated how disease spread changed when we varied the type and magnitude of mobility restrictions in different transmission scenarios, with variables such as the basic reproductive number ( $R_0$ ), length of infectious period, and the number of initial cases.

**Findings** 331 COVID-19 cases distributed across the ten regions of Shenzhen were reported on Feb 7, 2020. In our basic scenario ( $R_0$  of 2.68), mobility reduction of 20–60% within the city had a notable effect on controlling COVID-19 spread: a flattening of the peak number of cases by 33% (95% UI 21–42) and delay to the peak number by 2 weeks with a 20% restriction, 66% (48–75) reduction and 4 week delay with a 40% restriction, and 91% (79–95) reduction and 14 week delay with a 60% restriction. The effects of mobility restriction were increased when combined with reductions of 25% or 50% in transmissibility of the virus. In specific analyses of mobility restrictions for individuals with symptomatic infections and for high-risk regions, these measures also had substantial effects on reducing the spread of COVID-19. For example, the peak of the epidemic was delayed by 2 weeks if the proportion of individuals with symptomatic infections who could move freely was maintained at 20%, and by 4 weeks if two high-risk regions were locked down. The simulation results were also affected by various transmission parameters.

**Interpretation** Our model shows the effects of various types and magnitudes of mobility restrictions on controlling COVID-19 outbreaks at the city level in Shenzhen, China. The model could help policy makers to establish the optimal combinations of mobility restrictions during the COVID-19 pandemic, especially to assess the potential positive effects of mobility restriction on public health in view of the potential negative economic and societal effects.

**Funding** Guangdong Medical Science Fund, and National Natural Science Foundation of China.

**Copyright** © 2020 The Author(s). Published by Elsevier Ltd. This is an Open Access article under the CC BY 4.0 license.

## Introduction

In January 2020, an outbreak of COVID-19 began in Wuhan, China, and this disease spread rapidly to more than 200 countries.<sup>1</sup> COVID-19 is caused by a novel coronavirus known as severe acute respiratory syndrome coronavirus 2 (SARS-CoV-2), which has a very high transmissibility.<sup>2,3</sup> Restricting public mobility is a crucial public health tool to control respiratory infectious diseases. Such restrictions include physical distancing and community containment measures for reducing public transport use and public gatherings, school closures, and working from home where possible. Previous studies investigating influenza epidemics provided evidence for the small effects of these measures. For example, mobility restrictions were estimated to only reduce the peak number of individuals infected with H1N1 virus in local transmission by 10% and delay the peak incidence by 2 days.<sup>4</sup> However, this

scarcity of evidence is probably because such studies only captured information on some subpopulations, such as school children or people at work, not the whole population.<sup>5,6</sup>

In the context of COVID-19, mobility data including airline data and app-based data suggest that realistic travel restrictions at a national or even international level substantially mitigates disease spread between cities.<sup>2,7</sup> However, there is debate over what type and magnitude of mobility restrictions could be appropriate for controlling the COVID-19 outbreak. The optimal balance between the potential positive effects of mobility restrictions on public health and the adverse effects on freedom of movement, the economy, and society is unclear.

Mobile phone use in China among those aged 15–65 years is almost 100%; as such, mobile phone users can be considered representative of the entire

*Lancet Digital Health* 2020

2: e417–24

School of Public Health, Shenzhen University Health Science Center, Shenzhen, China (Y Zhou PhD, D Hu PhD); Institute for Advanced Study (R Xu MSc) and Guangdong Key Laboratory for Urban Informatics, Department of Urban Informatics (Y Yu PhD, Q Li PhD, J Xia PhD), Shenzhen University, Shenzhen, China; and Guangdong Laboratory of Artificial Intelligence and Digital Economy, Shenzhen, China (Y Yu, Q Li, J Xia)

Correspondence to:

Dr Jizhe Xia, Guangdong Key Laboratory for Urban Informatics, Department of Urban Informatics, Shenzhen University, Shenzhen 518000, China  
xjiazhe@szu.edu.cn

### Research in context

#### Evidence before this study

We searched PubMed and preprint archives for articles published in English that contained information about the COVID-19 pandemic published up to May 27, 2020, using the search terms “coronavirus”, “CoV”, “COVID-19”, “mobility”, “movement”, and “flow”. The data thus far suggests that realistic travel restrictions can substantially mitigate the spread of COVID-19 at the national and international level. However, because there is no complete picture of human community mobility patterns, it is unclear whether restricting mobility is effective at the city level and constitutes a proportionate response for controlling the COVID-19 outbreak.

#### Added value of this study

We built a susceptible–exposed–infectious–recovered transmission model for COVID-19 based on the city of Shenzhen, China. We harnessed mobile phone data, which reported human mobility patterns with an unprecedented level

of detail. We quantified the effect of controlling the COVID-19 outbreaks by the types (eg, general mobility restrictions, lockdown of high-risk regions, intraregion mobility restriction, or mobility restriction for infectious people) and magnitudes (eg, 20%, 40%, or 60%) of restriction interventions. These effects were greater when combined with measures to reduce viral transmission. The degree to which mobility restrictions at a certain level increase or decrease the epidemic size depends on the level of risk in the community and the characteristics of the COVID-19.

#### Implications of all the available evidence

The effect of different types and magnitudes of mobility restriction measures on controlling the COVID-19 outbreak was quantified in this study and could be modified with updated transmission characteristics. This model might aid policy makers in the management of the epidemic by predicting risk and assessing the effect of mobility restrictions at the city level.

population in this age group.<sup>8</sup> With this knowledge, we used anonymous aggregated mobile phone sightings data to build a COVID-19 transmission model for the Chinese city of Shenzhen.

## Methods

### Study design

In this modelling study, we combined the effects of intra-city mobility with the force of infection (ie, the rate at which susceptible individuals acquire an infectious disease) to predict the shape of the epidemic curve of COVID-19 in Shenzhen, China. We then assessed the effects on the shape of the epidemic curve when we simulated changes in type and severity of mobility restrictions and disease transmission suppression (eg, interventions such as using face coverings and improving personal hygiene) in the scenarios of various disease transmission parameters.

This study was approved by the Institutional Review Board of Shenzhen University. Personal privacy was strictly protected by using only anonymous and aggregated mobile phone data rather than individual records of travel or behaviour patterns. The anonymous and aggregated data was provided by the mobile phone service provider under the strict relevant laws and regulations. All data were supplied and analysed in an anonymous format, without access to personal identifying information. As such, the need for written consent from each mobile phone user was waived by the Institutional Review Board of Shenzhen University.

### Overview of the model

For this modelling study, we built a modified susceptible–exposed–infectious–recovered (SEIR) compartmental transmission model that categorised the

study population as follows: susceptible, vulnerable to SARS-CoV-2 infection; exposed, individuals exposed to the virus who are in the incubation period with no symptoms yet; infectious, symptomatic and capable of spreading the infection; or recovered, immune to infection or no risk of further infection. People newly infected and in the incubation period were assumed to be infectious because several studies have reported pre-symptomatic infections.<sup>9,10</sup> Models were constructed for each of Shenzhen’s ten administrative regions. By the model, COVID-19 could spread both within a region or between regions, mirroring the movement of people. The model design (appendix p 2) was similar to a previously described model to assess the dynamics of respiratory infectious diseases associated with human mobility.<sup>11</sup>

### Mobility data from mobile phone records

Mobile phone sightings data from working days (Monday to Friday) from Jan 10 to March 10, 2019, were provided by one of the leading mobile phone service providers in Shenzhen, China Unicom, which holds the records of more than 4 million anonymous subscribers. A user only needed to have their phone switched on (and not necessarily use it) for their location to be recorded. The origin–destination matrices were constructed by computing the number of people that move between different locations daily. The location where movements started between 0700 h to 0900 h were inferred as the resident location, because most people start their daily activities in the morning.<sup>12</sup> We considered the mobile phone data representative of the Shenzhen general population within the age range 15–65 years. We retrieved data on the borders of Shenzhen’s administrative divisions and the official

See Online for appendix

estimated population size of around 11 million (4·8% population growth from 2018) for 2020 from the Shenzhen Government website.<sup>13</sup>

### Characteristics of COVID-19

The daily number of confirmed cases of COVID-19 in Shenzhen was obtained from the Government website of Shenzhen, where all cases were organised by region of residence.<sup>14</sup> The incubation time for SARS-CoV-2 was 5·2 days (95% CI 4·1–7·0 days) and serial interval was 7·5 days (5·3–19).<sup>15</sup> Existing estimates of the basic reproductive number ( $R_0$ ) for COVID-19 vary widely from 1·9 to 6·5.<sup>16,17</sup> Similarly, the inferred duration of the infectious period of COVID-19 was from 6·5 to 21·0 days for various subpopulations.<sup>18</sup> Here, an  $R_0$  of 2·68 (2·47–2·86) and an infectious period of 12·7 days (9·4–26) was used for the basic scenario.<sup>2</sup> We applied various values for the  $R_0$  (4·0, 3·0, and 2·0), infectious period (15, 10, and 8 days) and initial number of cases (2, 5, and 15 times increases in initial cases) in the simulation analysis. Case definitions used by the local Government were obtained from the Chinese Centres for Disease Control (appendix p 1). The effective reproduction number ( $R_t$ ) in Shenzhen from Jan 10 to Feb 20, 2020, was estimated using the likelihood-based estimation method based on the observed dates for symptom onset using pairs of cases.<sup>19</sup> The hot areas (with high Getis-Ord spatial statistics values) in Shenzhen were established by daily incidence data, which analysed where features with either high or low values cluster spatially.<sup>20</sup>

### Transmission model structure

For the basic simulation, the confirmed cases reported in ten administrative regions at the start date (Feb 7, 2020) served as the number of infected cases for epidemic modelling—ie, at time ( $t$ )=0. A SEIR model was then built for the subpopulation constituting each of Shenzhen's ten regions. The model was built by using ordinary differential equations, such that for the  $i$ th region (with  $i$  from 1 to 10) where:

$$\frac{dS_i(t)}{dt} = -\lambda_i S_i(t)$$

$$\frac{dE_i(t)}{dt} = \lambda_i S_i(t) - \sigma_i E_i(t)$$

$$\frac{dI_i(t)}{dt} = \sigma_i E_i(t) - \gamma_i I_i(t)$$

$$\frac{dR_i(t)}{dt} = \gamma_i I_i(t)$$

$S_i(t)$ ,  $E_i(t)$ ,  $I_i(t)$ , and  $R_i(t)$  are the number of susceptible, exposed, infectious, and recovered individuals at time  $t$ . In the formula,  $\sigma_i$  corresponds to the inverse of the mean incubation period and  $\gamma_i$  was the recovery rate (the inverse of the mean infectiousness period), where an infected

patient recovers and is assumed to become immune to COVID-19 infection. The force of infection ( $\lambda$ ) in the  $i$ th region is:

$$\lambda_i = \sum_{j=1}^{k+1} m_{ij} \beta_j \frac{\sum_{l=1}^k m_{lj} (E_l + P_m I_l)}{\sum_{l=1}^k m_{lj} N_l}$$

Where  $N_l$  was the total population in the region  $l$ , and  $P_m$  represents the proportion of mobile infectious cases.  $\beta_j$  represents the transmission rate from infectious people and is estimated by dividing  $R_0$  by the infectious period. The entire population of Shenzhen was assumed to be susceptible. It was assumed that people in both the exposed and infectious categories had the same ability to infect susceptible people.

Mobile phone data was used to establish the number of people who were moving from region  $i$  to region  $j$  ( $L_{ij}$ ), including the number of people who were moving within region  $i$  with movement distance of more than 250 m ( $i=j$ ). Those who did not move further than 250 m in 1 day were presumed to be in home isolation, and the force of infection for these people was denoted as 0 ( $\beta_{\text{isolate}}=0$ ). Then, a  $K \times (K+1)$  mixing matrix  $M=\{m_{ab}\}$  was constructed, as follows:

$$\begin{cases} m_{ij} = \frac{L_{ij}}{N_i} \times \frac{8}{24}, 0 \leq i, j \leq K \\ m_{i, \text{isolate}} = 1 - \sum_{j=1}^K m_{ij}, 0 \leq i \leq K, \text{isolate} = K+1 \end{cases}$$

Where  $m_{ij}$  ( $1 \leq i, j \leq K$ ) is the average proportion of time that a resident of population  $i$  spends in population  $j$  on daily basis, and the  $m_{i, \text{isolate}}$  ( $1 \leq i \leq K, \text{isolate} = K+1$ ) is the proportion of time that a resident of population  $i$  is in home isolation. We assumed that the average time of stay in each movement was 8 h per day.

### Transmission scenarios

In the model, the magnitude of human mobility reduction in the city varied from 0% to 60%, at 20% intervals, to quantify the effect of general mobility restriction. The next set of scenarios thus modelled the effects of combining the graded restrictions in mobility (20–60%) with reduced disease transmissibility (at 25% and 50%). Some types of mobility restriction, including reducing the inter-region mobility for all regions or locking down high-risk regions by reducing their inter-region and intra-region mobility, were assessed in the model. The proportion of mobility for those in the infectious category was assumed to be 60% in the basic scenario; more than 25% of these people reported symptom onset before they travelled to Shenzhen from Hubei.<sup>14</sup> To quantify the effect of mobility restriction for those in the symptomatic infectious category (such as case isolation), simulations were established with the level of mobility set at 20%,

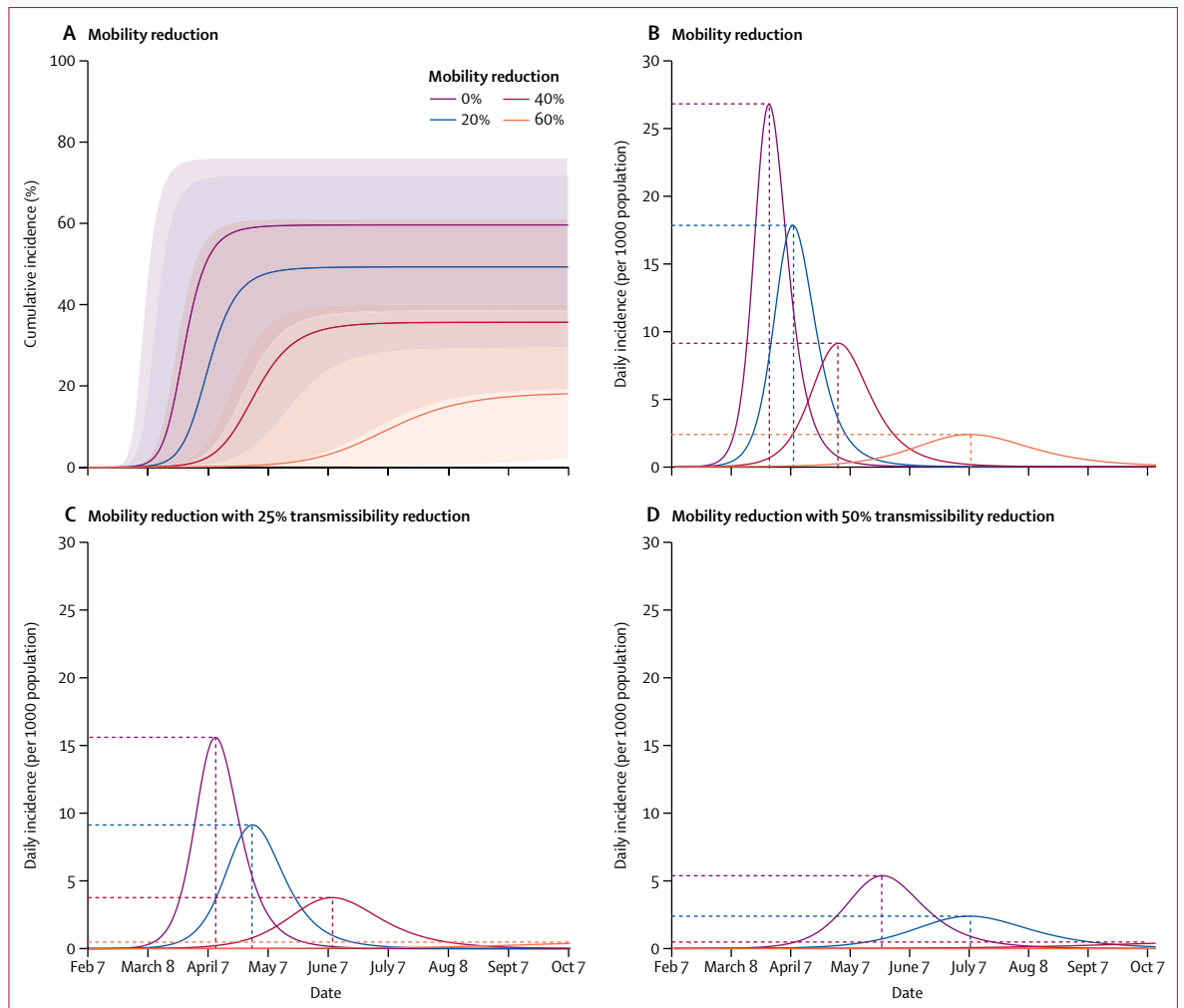


**Figure 1: Effects of human mobility restrictions in Shenzhen on COVID-19 incidence with and without transmissibility reduction, February to October, 2020** Cumulative incidence of COVID-19 (A) and daily incidence of COVID-19 (B) with varying mobility restrictions. Shaded areas in (A) are 95% uncertainty intervals. Daily incidence of COVID-19 with varying mobility restrictions with 25% reduction in transmissibility (C) and 50% reduction in transmissibility (D).

40%, or 60% for infectious people. No simulation was done for 0% mobility for the infectious category, because in real-world situations it is hard to control all symptomatic patients, including those with mild and moderate symptoms. The effect of mobility restriction was assessed in scenarios with various values of transmission and parameters of disease ( $R_0$ , duration of infectious period, and initial number of cases).

The effect of controlling the COVID-19 outbreak was investigated from two perspectives: (1) slowing the growth rate of the epidemic and (2) flattening the epidemic curve (ie, reducing the peak number of cases). We set a goal of no peak in the first half of 2020 (up to June 30) as the goal for infection control for comparison when applying different mobility restrictions. The 95% uncertainty intervals (UIs) were calculated using 1000 draws by bootstrap method for incubation period (log-normal distribution) and the serial interval ( $\gamma$  distribution). All

analyses were done with R version 3.6.2, ArcGIS version 10.5, and QGIS version 2.81.

### Role of the funding source

The funder of the study had no role in study design, data collection, data analysis, data interpretation, or writing of the report. The corresponding author had full access to all the data in the study and had final responsibility for the decision to submit for publication.

### Results

331 COVID-19 cases distributed across the ten regions of Shenzhen were reported on Feb 7, 2020 (Baoan [n=48], Nanshan [n=77], Futian [n=65], LuoHo [n=31], Yantian [n=3], Guangming [n=10], Longhua [n=31], Long Gang [n=58], Pingshan [n=6], and Dapeng [n=2]). We mapped these initial cases geographically, alongside the positions of the mobile phone base stations in Shenzhen

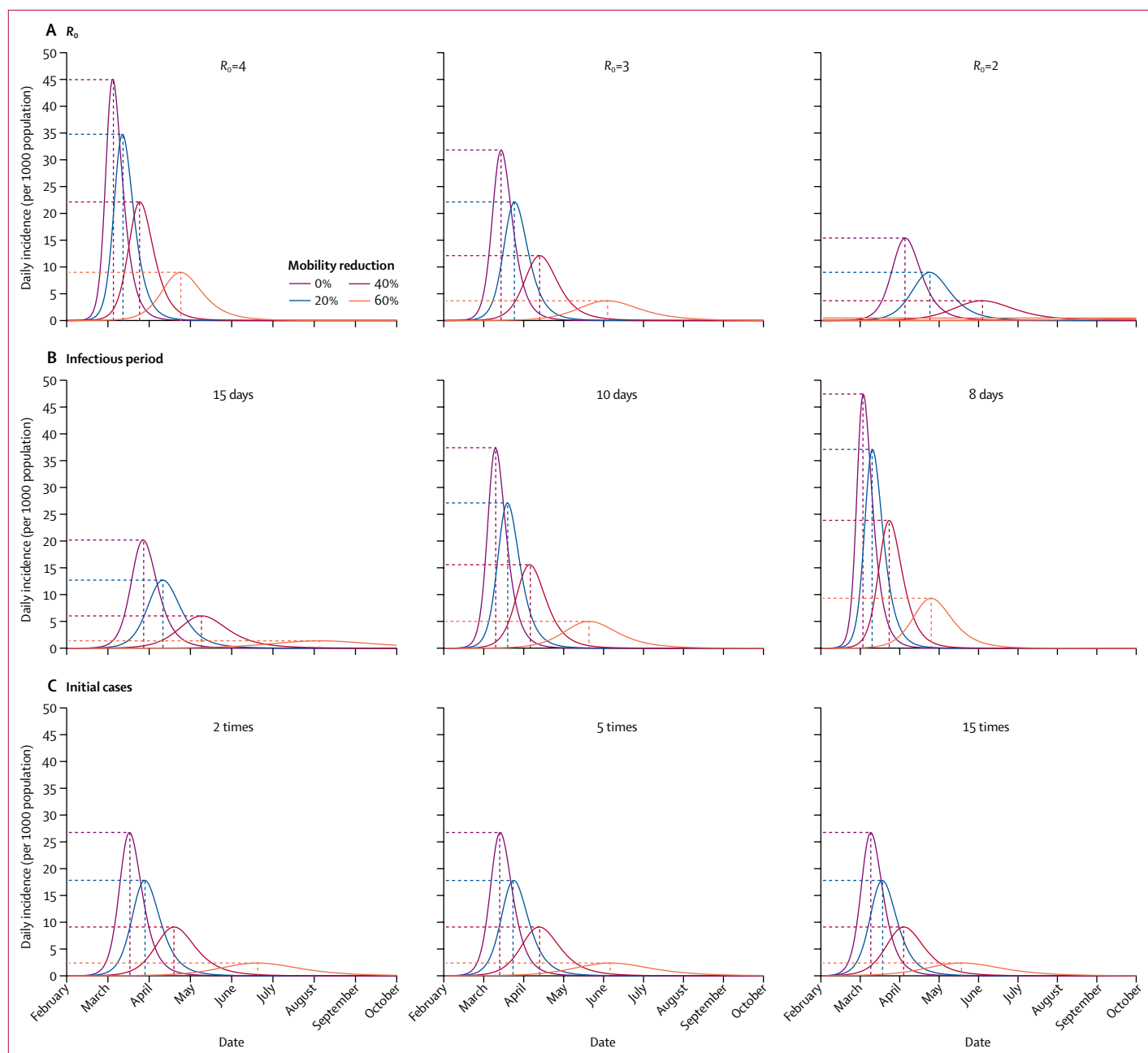


**Figure 2: Effects of mobility restrictions on COVID-19 incidence under different transmission scenarios, February to October, 2020**

Daily incidence of COVID-19 with varying mobility restrictions and a varied reproduction number (A), infectious period (B), and initial numbers of cases in Shenzhen (C). The baseline scenario is an  $R_0$  of 2.68, an infectious period of 12.7 days, and 331 initial cases in the city.  $R_0$ =basic reproductive number.

(appendix p 3). Alongside, we provide the actual local spread of COVID-19 in Shenzhen (appendix p 4). Most cases were imported from Wuhan; minimal local community transmission occurred in the city. The  $R(t)$  was less than 1.0 within 2 weeks after the first imported case was reported because of a series of immediate public health interventions being implemented (appendix p 4).

In the simulated basic scenario ( $R_0$  of 2.68; figure 1), the Shenzhen epidemic was predicted to peak in March,

2020, in the absence of any public health interventions. If intra-city mobility was reduced by 20%, the epidemic peak would be delayed for about 2 weeks and the peak incidence would decrease by about 33% (95% UI 21–42). With a moderate (25%) reduction in disease transmissibility, a 20% mobility reduction (vs no mobility reduction) further delayed the epidemic peak, by around 4 weeks, and the peak incidence of the epidemic decreased by 42% (29–48; figure 1C). A 40% reduction in intracity mobility

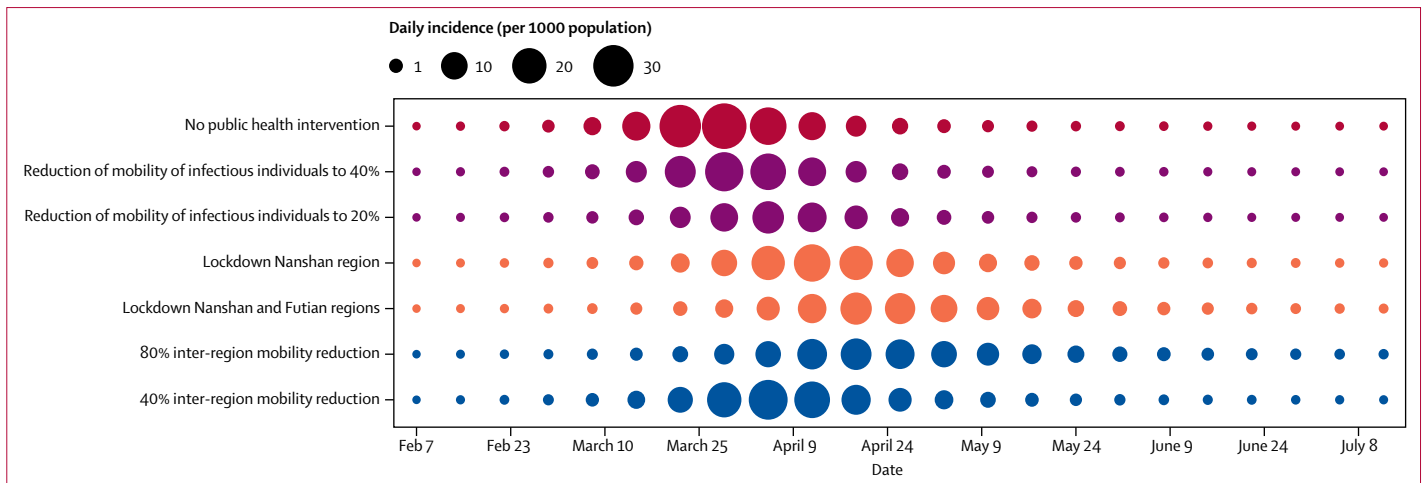


Figure 3: Effects of various mobility restrictions for subgroups and high-risk regions on COVID-19 incidence, February to July, 2020

would delay the peak by 4 weeks and reduce the peak daily incidence by around 66% (48–75). A 40% reduction in intracity mobility in conjunction with a moderate (25%) reduction in disease transmissibility delayed the peak by 7 weeks, and the magnitude of the epidemic dropped by 76% (61–82). A 60% reduction delayed the peak by 14 weeks, and decreased the magnitude of the epidemic by 91% (79–95). Notably, if 60% mobility reduction was combined with 25% reduction in disease transmissibility, the epidemic would grow slowly without peaking in the first half of 2020. The effectiveness of reduced mobility (20–60%) was greatest when combined with a strong (50%) reduction in transmissibility.

The effect of reducing mobility varied under different disease transmission conditions, including basic reproduction number, infectious period, and number of initial cases (figure 2). For example, the peak reduction effects were greatest for all levels of mobility reduction when  $R_0$  was 2.0, and the peak was fastest and highest when  $R_0$  was close to 4.0. Specifically, the model showed that a 60% reduction in mobility could prevent a peak from occurring during the first half of 2020 in the scenario with an  $R_0$  of 2.0; resulting in a peak occurring in the second week of June with an estimated peak number of four cases per 1000 population in the scenario with  $R_0$  of 3.0; or cause the epidemic peak to occur within the first week of May with an estimated peak number of cases of nine per 1000 population in the scenario with  $R_0$  of 4.0. At a given  $R_0$ , a longer infectious period was associated with lower transmissibility because the  $R_0$  is essentially proportional to the product of the infectious period and transmissibility. Therefore, 60% mobility reduction could be closer to the goal of preventing a peak in the first half of the year when the infectious period was 15 days rather than when the infectious period was 10 days or 8 days. Notably, increasing the initial number of cases 2–15-times could accelerate the

arrival of the epidemic peak by 2–3 weeks but had a negligible effect on the magnitude of the epidemic.

We assessed the effects of mobility reduction for subgroups or regions (figure 3). If the proportion of individuals in the infectious category who could move freely was controlled at 20%, the epidemic could be delayed by 2 weeks and the peak number of cases could be reduced by 50% compared with a no public health intervention scenario. If inter-region mobility was reduced by 80%, the peak of the epidemic could be delayed by around 4 weeks and the peak number of cases could be reduced by 50% compared with a no public health intervention scenario. We also simulated the effects of locking down two regions with the highest number of initial cases (Nanshan and Futian). The epidemic peak could be delayed by 4 weeks. Furthermore, the effect of the mobility reduction could be substantially affected by  $R_0$  (appendix p 5).

## Discussion

Mobility restriction is an important public health tool and has been used globally to control the COVID-19 pandemic. In this study, we used anonymous and aggregated mobile phone sightings data to establish the transmission dynamics of COVID-19 in a megacity (Shenzhen) in China. Our simulation reflected the potential effect of different types and magnitudes of human mobility restriction measures on controlling the spread of COVID-19. Mobility restriction measures could be more effective if combined with transmissibility reduction measures. The effects of mobility reductions were also greatly affected by the transmission characteristics of the disease itself, which need further exploration in future studies.

We built a transmission model that considers human mobility patterns derived from anonymous and aggregated mobile phone data, which is expected to change

epidemiology.<sup>21,22</sup> To date, available mobility data (including data from air and rail travel authorities, GPS loggers, apps or social media sources) could only capture the trajectories of subpopulations who use specific transport tools or install specific applications on their mobile phones.<sup>23</sup> By contrast, the almost 100% coverage of mobile phone use in the population aged 15–65 years means that anonymous mobile phone data are: (1) more representative for the whole population and (2) an accurate reflection of overall movement patterns on various spatial and temporal scales.<sup>24</sup> Therefore, mobile phone data can be a vital resource to understand the transmission dynamics of infectious diseases such as COVID-19 in the context of human mobility.<sup>25,26</sup>

Although public health interventions might differ at different stages of the outbreak, our model provides information in the different epidemiological processes. In the acceleration stage of the pandemic when incidence increases exponentially, the foci become the public health interventions for containment. Our model is important to assess how various types and magnitudes of mobility restriction interventions might have affected the spread of COVID-19 in Shenzhen, especially to find the optimal combination of the interventions (eg, general mobility restrictions, lockdown of high-risk regions, or intra-region mobility reduction) and magnitudes (eg, 20%, 40%, or 60% restriction) of interventions at the right time. Our model could also help policy makers to balance the potential benefit of mobility restriction along with any potential negative societal and economic costs.<sup>27</sup> In the deceleration stage or after the epidemic, our model could be modified to assess the effect of realistic interventions on the progression of COVID-19 in future.

In the basic scenario that we modelled ( $R_0$  of 2.68), the epidemic in Shenzhen was predicted to peak around March, 2020, with daily incidence of 27 per 1000 population. Mobility reduction of 20–60% within the city had a notable effect on controlling COVID-19 spread: a flattening of the peak number of cases by 33–90% and a delay in the forward trajectory of the epidemic by 2–14 weeks. With a 60% reduction in mobility, no obvious peak occurred in the first half of 2020 if combined with 25% transmissibility reduction. The transmissibility reduction measures have substantial effects on the control of COVID-19 outbreaks (appendix p 4), but would be more effective if combined with mobility reduction measures. In practice, the world has witnessed various mobility reduction strategies applied to some subgroups (eg, reducing the mobility of infectious individuals with symptoms by isolation or admission to hospital) or regions (eg, lockdown in high-risk regions). The lockdown measures imposed on Wuhan substantially mitigated the spread of COVID-19 to other cities.<sup>28</sup> In our model, a lockdown in high-risk regions within a city can have a substantial effect on controlling local transmission of COVID-19 in that city.

When the value of  $R_0$  increased, a higher proportion of the mobility reduction needed to be implemented to

achieve the same goal. Numbers of initial cases had a minor effect on the extent of local outbreaks, which is consistent with previous reports that suggested the prevention of movement in Wuhan would have had a negligible effect on local transmission in other cities because the increasing number of initial infections was substantially smaller than the size of the susceptible population in the megacities.<sup>27</sup> We set a goal of achieving no peak of infection in the first half of the year for comparison; others have defined their disease control target as achieving no peak within 3 months.<sup>26</sup> Policy makers worldwide are still trying to use this paradigm when setting their goals for controlling the outbreak of COVID-19,<sup>27</sup> but goals depend on availability of medical resources or management policies. Our model can be modified further to reflect other specific definitions of outbreak control.

Our study has several major limitations that must be noted. First, the  $R(t)$  was controlled to less than 1.0 within 2 weeks after the first case was detected in Shenzhen. Therefore, it was impossible for us to validate our model using the real spread data. However, the modelling techniques that we used in this study are very similar to a previous study on the epidemic dynamic of influenza.<sup>11</sup> Second, the mobility data that we used from 2019 might not necessarily reflect mobility patterns in 2020. Third, the mobile phone data we used in this analysis was from one of the leading operator companies and was extrapolated to represent the whole population flow in the city. Due to scarcity of demographic information for the floating population (ie, migrants with no local household registration), who account for about 65% of the whole population in Shenzhen,<sup>29,30</sup> it is unclear whether demographic distributions of mobile phone users are proportional to the distributions of the whole population in the city. However, by covering the floating population, the mobile phone data made it possible to assess human mobility in Shenzhen. Fourth, our model did not include asymptomatic infections; thus, outbreak size might have been underestimated if there were many highly infectious individuals, but these data are unknown.<sup>3</sup> The transmission parameters in our model, such as  $R_0$ , infectious period, serial interval (ie, the time between successive cases in a chain of transmission), and mobility reduction for infectious individuals had substantial effects on the results of our model. However, a precise understanding of COVID-19 transmission characteristics is an area that still requires further research. Additionally, our model assumed that individuals in the exposed category were infectious and had similar infectiousness as the infectious category. Assuming that these individuals were less infectious would decrease the size of the COVID-19 epidemic curve. We simplified our model to establish the effect of mobility restrictions on the control of outbreaks; however, as more reliable scientific evidence becomes available, the model can be updated in future.



In summary, our modelling based on population dynamics in Shenzhen, China, suggests that human mobility restrictions in the city had a large effect on controlling the COVID-19 outbreak, especially when implemented in conjunction with efforts to reduce transmissibility. This model could be modified in future, as more information comes to light on COVID-19 transmission characteristics. This model might provide evidence to policy makers and planners to help manage COVID-19 outbreaks worldwide.

#### Contributors

YZ ran the study, analysed and interpreted data, wrote the paper, and obtained funding for the study. JX extracted the data, analysed and interpreted data, and obtained funding for the study. RX analysed and interpreted data. QL participated in discussions and obtained funding for the study. DH and YY participated in discussions on conducting the study. All authors reviewed the paper for content and approved the final report.

#### Declaration of interests

We declare no competing interests.

#### Data sharing

We collated epidemiological data from publicly available data sources (Shenzhen government website). All the epidemiological information that we used is documented in the Article. We purchased the mobile phone sightings data from January to March, 2019, data from the service provider (China Unicom). Our data purchase agreement with China Unicom prohibits us from sharing these data with third parties, but interested parties can contact China Unicom to make the same data purchase.

#### Acknowledgments

We thank Zhucheng Zhang and Shuting Yang from Shenzhen University (Shenzhen, China) for assistance with data collection and technical assistance. This work has received financial support from the Guangdong Medical Science Fund (grant no A2019015) and National Natural Science Foundation of China (grant no 41701444, 71961137003).

#### References

- 1 WHO. Coronavirus disease 2019 (COVID-19) situation report—54. March 14, 2020. <https://www.who.int/emergencies/diseases/novel-coronavirus-2019/situation-reports> (accessed March 15, 2020).
- 2 Wu JT, Leung K, Leung GM. Nowcasting and forecasting the potential domestic and international spread of the 2019-nCoV outbreak originating in Wuhan, China: a modelling study. *Lancet* 2020; **395**: 689–97.
- 3 Bai Y, Yao L, Wei T, et al. Presumed asymptomatic carrier transmission of COVID-19. *JAMA* 2020; **323**: 1406–07.
- 4 Frias-Martinez E, Williamson G, Frias-Martinez V. An agent-based model of epidemic spread using human mobility and social network information. Institute of Electrical and Electronics Engineers. 2011. <https://ieeexplore.ieee.org/stamp/stamp.jsp?tp=&arnumber=6113095> (accessed May 27, 2020).
- 5 Fong MW, Gao H, Wong JY, et al. Nonpharmaceutical measures for pandemic influenza in nonhealthcare settings—social distancing measures. *Emerg Infect Dis* 2020; **26**: 976–84.
- 6 Markel H, Lipman HB, Navarro JA, et al. Nonpharmaceutical interventions implemented by US cities during the 1918-1919 influenza pandemic. *JAMA* 2007; **298**: 644–54.
- 7 Chinazzi M, Davis JT, Ajelli M, et al. The effect of travel restrictions on the spread of the 2019 novel coronavirus (2019-nCoV) outbreak. *medRxiv* 2020; published online Feb 11. <https://doi.org.10.1101/2020.02.09.20021261> (preprint).
- 8 Deloitte. Chinese consumers at the forefront of digital technologies: China Mobile Consumer Survey 2018. <https://www2.deloitte.com/content/dam/Deloitte/cn/Documents/technology-media-telecommunications/deloitte-cn-2018-mobile-consumer-survey-en-190121.pdf> (accessed April 26, 2020).
- 9 Hou C, Chen J, Zhou Y, et al. The effectiveness of quarantine of Wuhan city against the Corona Virus Disease 2019 (COVID-19): a well-mixed SEIR model analysis. *J Med Virol* 2020; **92**: 841–48.
- 10 Yu P, Zhu J, Zhang Z, Han Y. A familial cluster of infection associated with the 2019 novel coronavirus indicating possible person-to-person transmission during the incubation period. *J Infect Dis* 2020; **221**: 1757–61.
- 11 Wu JT, Riley S, Leung GM. Spatial considerations for the allocation of pre-pandemic influenza vaccination in the United States. *Proc Biol Sci* 2007; **274**: 2811–17.
- 12 Yuan JY, Zheng Y, Xie X. Discovering regions of different functions in a city using human mobility and points of interest. In: Thill JC (ed). *Spatial analysis and location modeling in urban and regional systems. Advances in geographic information science*. Berlin: Springer, 2017: pp 33–62.
- 13 Shenzhen Statistics Department. Bulletin of main statistics from the national census in Shenzhen. 2018 (in Chinese). <http://tjj.sz.gov.cn/ztlz/ztsjfb/> (accessed March 3, 2020).
- 14 Shenzhen Government. Data about COVID-19. 2020 (in Chinese). [https://opendata.sz.gov.cn/data/dataSettoDataDetails/29200\\_01503668](https://opendata.sz.gov.cn/data/dataSettoDataDetails/29200_01503668) (accessed Feb 26, 2020).
- 15 Li Q, Guan X, Wu P, et al. Early transmission dynamics in Wuhan, China, of novel coronavirus-infected pneumonia. *N Engl J Med* 2020; **382**: 1199–207.
- 16 Liu Y, Gayle AA, Wilder-Smith A, Rocklöv J. The reproductive number of COVID-19 is higher compared to SARS coronavirus. *J Travel Med* 2020; **27**: taaa021.
- 17 Shao N, Cheng J, Chen W. The reproductive number R0 of COVID-19 based on estimate of a statistical time delay dynamical system. *medRxiv* 2020; published online Feb 20, 2020. <https://doi.org/10.1101/2020.02.17.20023747> (preprint).
- 18 Byrne AW, McEvoy D, Collins A, et al. Inferred duration of infectious period of SARS-CoV-2: rapid scoping review and analysis of available evidence for asymptomatic and symptomatic COVID-19 cases. *medRxiv* 2020; published online April 30, 2020. <https://doi.org/10.1101/2020.04.25.20079889> (preprint).
- 19 Wallinga J, Teunis P. Different epidemic curves for severe acute respiratory syndrome reveal similar impacts of control measures. *Am J Epidemiol* 2004; **160**: 509–16.
- 20 Songchitruksa P, Zeng X. Getis–Ord spatial statistics to identify hot spots by using incident management data. *Transp Res Rec* 2010; **2165**: 42–51.
- 21 González MC, Hidalgo CA, Barabási A-L. Understanding individual human mobility patterns. *Nature* 2008; **453**: 779–82.
- 22 Wesolowski A, Metcalf CJE, Eagle N, et al. Quantifying seasonal population fluxes driving rubella transmission dynamics using mobile phone data. *Proc Natl Acad Sci USA* 2015; **112**: 11114–19.
- 23 Finger F, Genolet T, Mari L, et al. Mobile phone data highlights the role of mass gatherings in the spreading of cholera outbreaks. *Proc Natl Acad Sci USA* 2016; **113**: 6421–26.
- 24 Mine T, Fukuda A, Ishida S. Intelligent transport systems for everyone's mobility. Singapore: Springer, 2019: pp 1–26.
- 25 Wesolowski A, Eagle N, Tatem AJ, et al. Quantifying the impact of human mobility on malaria. *Science* 2012; **338**: 267–70.
- 26 Wesolowski A, Zu Erbach-Schoenberg E, Tatem AJ, et al. Multinational patterns of seasonal asymmetry in human movement influence infectious disease dynamics. *Nat Commun* 2017; **8**: 2069.
- 27 Ferguson NM, Laydon D, Nedjati-Gilani G, et al. Impact of non-pharmaceutical interventions (NPIs) to reduce COVID-19 mortality and healthcare demand. March 16, 2020. <https://www.imperial.ac.uk/media/imperial-college/medicine/sph/ide/gida-fellowships/Imperial-College-COVID19-NPI-modelling-16-03-2020.pdf> (accessed March 20, 2020).
- 28 Lau H, Khosrawipour V, Kocbach P, et al. The positive impact of lockdown in Wuhan on containing the COVID-19 outbreak in China. *J Travel Med* 2020; **27**: taaa037.
- 29 Liang Z, Ma Z. China's floating population: new evidence from the 2000 census. *Popul Dev Rev* 2004; **30**: 467–88.
- 30 Shenzhen Statistics Department. Shenzhen statistics yearbook 2019 (in Chinese). [https://www.sz.gov.cn/sztjj2015/zwgk/zfxxgkml/tjsj/tjnj/201912/t20191230\\_18956670.htm](https://www.sz.gov.cn/sztjj2015/zwgk/zfxxgkml/tjsj/tjnj/201912/t20191230_18956670.htm) (accessed May 3, 2020).